JOURNAL OF GEOPHYSICAL RESEARCH, VOL. 101, NO. B11, PAGES 25,437-25,457, NOVEMBER 10, 1996

Geometry of the 1954 Fairview Peak-Dixie Valley earthquake sequence from a joint inversion of leveling and triangulation data

Kathleen M. Hodgkinson, Ross S. Stein, and Grant Marshall[1]
U.S. Geological Survey, Menlo Park, California

Abstract. In 1954, four earthquakes greater than M_S=6.0 occurred within a 30-km radius and in a period of 6 months. Elevation and angle changes calculated from repeated leveling and triangulation surveys which span the coseismic period provide constraints on the fault geometries and coseismic slip of the faults which were activated. The quality of the coseismic geodetic data is assessed. Corrections are applied to the leveling data for subsidence due to groundwater withdrawal in the Fallon area, and a rod miscalibration error of 150±30 ppm is isolated in leveling surveys made in 1967. The leveling and triangulation observations are then simultaneously inverted using the single value decomposition (SVD) inversion method to determine fault geometries and coseismic slip. Using SVD, it is possible to determine on which faults slip is resolvable given the data distribution. The faults are found to dip between 50° and 80° and extend to depths of 5 to 14 km. The geodetically derived slip values are generally equal to, or greater than, the maximum observed displacement along the surface scarps. Where slip is resolvable the geodetic data indicates the 1954 sequence contained a significant component of right-lateral slip. This is consistent with the N15°W trending shear zone which geodetic surveys have detected in western Nevada.

Introduction

Dixie Valley is a northeast trending valley, 80 km long and at most 24 km wide, situated in western Nevada. It is bordered on the west by the Stillwater Range and to the east by the Clan Alpine Range (Figure 1). The mountains rise over a kilometer above the valley floor. The 1954 earthquake sequence ruptured the Dixie Valley, Fairview, Rainbow Mountain, West Gate and Gold King faults (Figure 1). The series began with two events on the Rainbow Mountain fault on July 6 (M=6.6) and August 24 (M=6.8), 1954. On December 16, 1954, an M=7.1 event occurred on the Fairview fault [*Doser,* 1986]. The West Gate and Gold King faults ruptured simultaneously [*Doser,* 1986]. Four minutes and twenty seconds after the Fairview Peak earthquake, the Dixie Valley fault ruptured (M=6.8) [*Doser,* 1986]. The events produced a zone of ruptures almost 100 km long. The 1954 earthquake sequence is one of only three cases of normal faulting earthquakes in the Basin and Range province recorded geodetically, the M_S=6.9 1983 Borah Peak and M_S=7.3 1959 Hegben earthquakes being the other two. The sequence thus provides a rare opportunity to study geodetically the subsurface structure of active Basin and Range faults.

The aim of this paper is to identify the geometry of the faults and the coseismic slip associated with each event. This is accomplished by inverting the geodetic data and assuming the surface deformation can be described by simple models of uniform slip on planar faults embedded in and elastic-half space. The coseismic fault geometries which best fit the leveling and triangulation data simultaneously in the least squares sense are determined and then the triangulation and leveling data are inverted simultaneously for coseismic slip associated with all the major earthquakes.

To construct reliable source models for the earthquakes, the data quality must be assessed, systematic errors must be isolated, and nontectonic signals removed. Inconsistencies in the postseismic data leveling data in the Fairview Peak area have cast doubt on its reliability [*Savage and Church,* 1974] and suggest that systematic errors contaminate the postseismic leveling data. It was therefore necessary to establish that the inconsistent trends were a systematic error and determine which survey contained the error. Using leveling data not previously analyzed, it was possible to do this.

Previous Work

Previous studies of the geodetically measured 1954 coseismic deformation have involved separate analysis of leveling and triangulation data sets. *Savage and Hastie* [1969] inverted triangulation and leveling data separately to determine the coseismic slip and fault geometry of the Fairview fault. The data consisted of absolute elevation changes at benchmarks and displacement vectors which were derived from the triangulation measurements by *Whitten* [1957]. Deformation caused by the Dixie Valley earthquake and rupture of the nearby West Gate and Gold King faults was not taken into account in the analysis. Both leveling and triangulation data indicated a fault of width of 8 km, strike of N9°E and dip of 57±6°E (Table 1). The strike of the model fault was consistent with the orientation of scarps which trended a few degrees east of north but not consistent with the

[1]Now at Trimble Navigation Limited, Sunnyvale, California.

Paper number 96JB01643.
0148-0227/96/96JB-01643$09.00

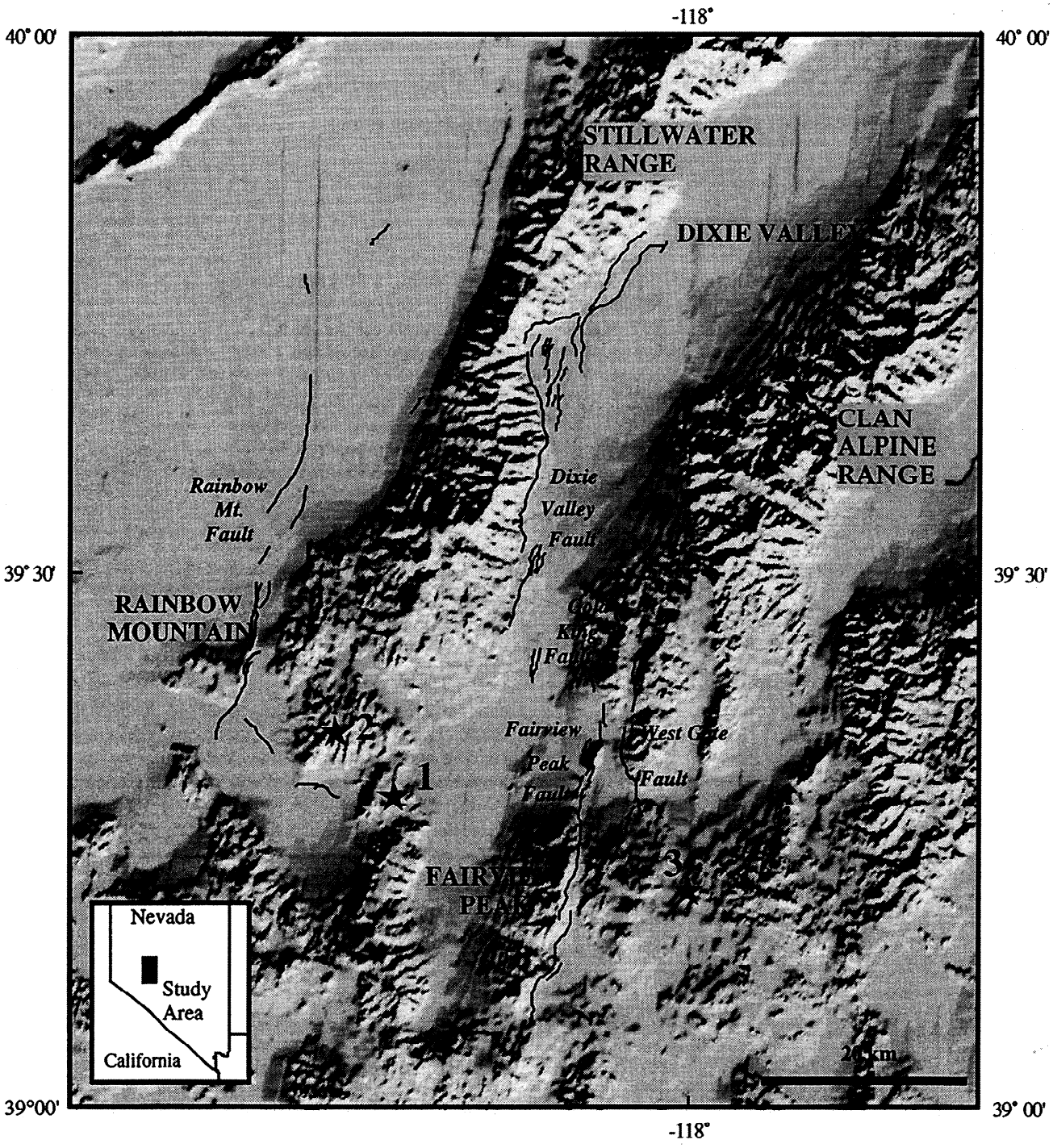

Figure 1. Map of the study area. The fault ruptures are shown as black lines. The direction of slip is indicated by arrows and the dip by dots on the faults. Epicenters are marked by stars and numbered in the order in which the earthquakes occurred [*Doser*, 1986]. Inset shows the location of the study area within Nevada.

focal mechanism of the Fairview Peak earthquake which gave a strike of N10°W (Table 2) [*Doser*, 1986]. The triangulation data were fit best by 2.9±0.4 m of right-lateral and 2.3±0.4 m of vertical slip (Table 1). The leveling data were best fit by 2.8±0.1 m of vertical slip.

Snay et al. [1985] estimated fault geometry and coseismic slip for all the major earthquakes in the sequence by modeling the coseismic shear strain within the Rainbow Mountain-Fairview Peak-Dixie Valley triangulation network. The observations were derived by minimally constraining motion at points at the extremity of the network. Some fault parameters such as lower depths had to be constrained to a fixed value in the analysis. Deformation around Fairview Peak was best fit by assuming a two-fault structure where a shallow fault with bottom depth 5 km overlay a deeper fault of bottom depth of 20±50 km (Table 1). While the strike of the upper fault was similar to that of the surface scarps, the lower fault had a strike of 1° to 13° west of north. Right-lateral slip of 3.6±0.4 m and 0.8±0.4 m and vertical slip of 2.3±0.5 m and 1.6±0.7 m were determined on the upper and lower faults

Table 1. Fault Parameters and Coseismic Slip Derived by *Savage and Hastie* [1969] and *Snay et al.* [1985] for the Fairview Peak, West Gate, Gold King, Dixie Valley, and Rainbow Mountain Earthquakes

Fault	Displacement, m		Length, km	Strike	Dip	Width, km
	Horizontal	Vertical				
Savage and Hastie [1969]						
Fairview Peak	2.9±.04	2.3±0.4	50	N9°E	57±6°E	8.0±2.0
Snay et al. [1985]						
Fairview Peak (shallow)	3.6±.04	2.3±0.5	34±4	N12±3°E	63±10°E	5.0±1.5
Fairview Peak (deep)	0.8±0.4	1.6±0.7	58±40	N13±7°W	59±17°E	20±2.0
West Gate-Gold King	1.3±0.5	0.5±1.0	23±16	N7±3°E	70±23°W	5.0*
Dixie Valley	-0.3±1.1	2.4±1.6	42*	N6±17°E	60°E*	15.0*
Rainbow Mountain	0.6±.06	5.5±3.0	112*	N7±7°E	68±5°E	7.0±3.0

* Constrained to this value during modeling.

respectively. A hypothetical fault between the Rainbow Mountain fault and the Dixie Valley fault was required to fit the data west of the Stillwater Range. The vertical motion required on the hypothetical sixth fault, however, 1.8 m, is not inferable from the coseismic leveling data. The West Gate and Gold King faults were modeled as one fault. The combined fault dipped steeply to the west at 70°±23°W to 80°±13°W and the bottom depth was constrained to 5 km. Only the strike and coseismic slip of the Dixie Valley fault were determined, the other parameters being constrained to fixed values (Table 1).

In this study, angle changes at triangulation stations are modeled rather than derived from quantities such as the displacement or strain fields. These are direct observations, no points need to be fixed or minimally constrained during the coseismic period to calculate the coseismic angle changes. Thus errors caused by rotation or dilation of the network are avoided. In modeling the leveling data, the relative elevation changes between adjacent benchmarks are used. Datum offsets between the pre- and postseismic surveys, which introduce biases to the absolute elevation changes, are then avoided.

Observed Surface Offsets and Focal Mechanisms of the Earthquakes

The focal mechanism of the first Rainbow Mountain event indicated it was a right-lateral faulting earthquake (Table 2) [*Doser*, 1986]. The scarp trended N15°E and was uplifted on the west side. The maximum vertical displacement measured was 0.3 m (Table 2) [*Tocher*, 1956]. The second event on the Rainbow Mountain fault caused rupture on the northern part of the fault and created an additional 20 km of surface rupture [*Tocher*, 1956]. Recent mapping of the Rainbow Mountain fault scarps indicates that a maximum of 0.9 m right-lateral motion along the Rainbow Mountain fault (S.J. *Caskey*, personal communication, 1996). The focal mechanism of the second earthquake shows right-lateral oblique slip along a fault plane striking N25°E and dipping 55°E [*Doser*, 1986] (Table 2). A focal depth of 10 to 12 km was estimated for the events from body wave modeling [*Doser*, 1986].

Fault plane solutions of the Fairview Peak earthquake indicate a fault striking N10°W and dipping 60°E [*Doser*, 1986]. A right-lateral component of slip almost twice as large as the normal is evident in the focal mechanism [*Doser*, 1986; *Romney*, 1957]. The focal depth, estimated from P-pP arrivals,

Table 2. Geological and Seismological Parameters Derived for the 1954 Earthquakes

Fault	Geological Parameters				Seismological Parameters	
	Displacement, m		Dip	Strike	Depth, km	strike/dip/rake
	Horizontal	Vertical				
Rainbow Mountain	0.9[a]	0.3[b]	East	N15°E	10±1[c]	336/80/-140(±5)[c]
					12±1[d]	355/50/-145(±5)[d]
Fairview Peak	2.9 (1.00)[e]	3.8 (1.20)[e]	55°-75°E	N12°E	15±2	350/60/-145(±5)
West Gate	1.2 (0.60)[e]	1.2 (0.40)[e]	West	N10°E		
Gold King	0.0[e]	1.0 (0.45)[e]	West	N10°E		
Dixie Valley	0.0[e]	2.8 (0.90)[e]	55°-75°E	N10°E	12±3	350/50/-90(±20)

The maximum displacements found at single points along the fault scarps are given and the average displacements, where available, are shown in parentheses. The seismological parameters are those derived from teleseismic analysis [*Doser*, 1986].

[a] S.J. Caskey, (personal communication, 1996) (vertical ground separation is shown),

[b] *Tocher* [1956]

[c] July 6 Rainbow Mountain

[d] August 24 Rainbow Mountain

[e] *Caskey et al.* [1996]

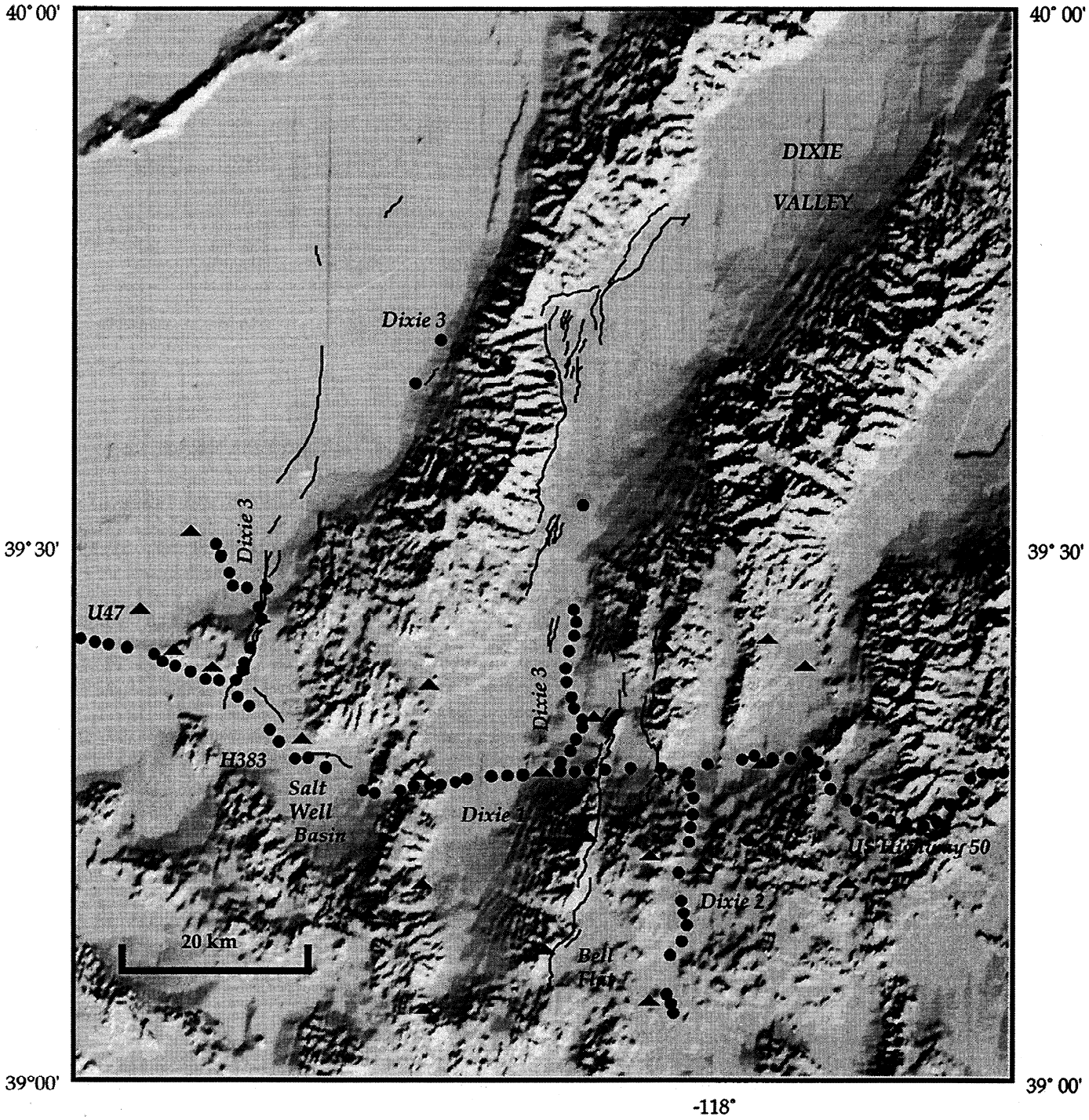

Figure 2. The geodetic data distribution. Dots denote leveling bench marks, and triangles denote triangulation stations. Leveling routes are indicated by Dixie 1, Dixie 2, and Dixie 3.

was 15±2 km [*Doser*, 1986]. The scarp dipped between 55° and 75° east and trended N10°E [*Slemmons*, 1957]. Vertical and right-lateral offsets were greatest at Fairview Peak where they were 3.8 m and 2.9 m, respectively [*Caskey et al.*, 1996].

The West Gate fault scarp dips to the west and is 19 km long (Figure 1). The maximum right-lateral and vertical offsets were about 1.2 m (Table 2). The westward dipping Gold King fault scarp extends for 12 km as a discontinuous group of fractures [*Caskey et al.*, 1996]. Vertical offsets along the rupture ranged from 0.2 to 1.0 m. No right-lateral displacements were observed along the Gold King fault [*Caskey et al.*, 1996].

The Dixie Valley earthquake created 50 km of fault scarps which dipped 50° to 70° to the east [*Bell and Katzer*, 1991]. The best fit to the teleseismic waveforms from the event was that of normal slip on a fault striking N10°W and dipping 60°E at a depth of 12±3 km [*Doser*, 1986]. The maximum vertical offset observed was 2.8 m and between 0.25 and 1 m of slip

was observed on a piedmont fault a few kilometers east of the Dixie Valley fault [*Caskey et al.*, 1996]. No right-lateral offsets were observed [*Caskey et al.*, 1996].

Geodetic Data

The Leveling Data

Leveling measures the relative height differences between points along a horizontal line of sight. Measurements are made with graduated rods which must be vertical, stable, and precisely calibrated. One measurement is called a setup, and the line between two permanent bench marks is called a section. Prior to 1970, most leveling lines were double run, i.e., each section was leveled once in a forward and then in a backward direction. Standards for leveling fall into three orders: first, second and third, each with class subdivisions. The most precise leveling is first order. Each order has tolerances that must be met and measurement procedures to be followed.

There are three leveling routes in the Dixie Valley area (Figure 2). The main leveling route is an east-west line along U.S. Highway 50 and is referred to as Dixie 1. The line lies almost perpendicular to the 1954 fault scarps. The second route, referred to as Dixie 2, begins on US Highway 50, and runs south along the eastern flank of Fairview Peak. The third route, called Dixie 3, begins on U.S. Highway 50 and runs north into Dixie Valley paralleling the Dixie Valley fault scarp. It crosses the Stillwater Range and continues south through Carson Sink paralleling the Rainbow Mountain fault scarp. Routes Dixie 1 and 2 were surveyed in 1934 and have been resurveyed five times since 1954 (Table 3). The Dixie 3 lines was surveyed twice before the events and has since been resurveyed three times (Table 3).

Water Withdrawal in Carson Sink

Elevation changes between 1934, 1955, 1967, and 1986 along the Dixie 1 route indicate subsidence caused by water withdrawal may be occurring between 20 km and 60 km (Figure 3). This subsidence is observed as negative elevation change with respect to benchmark H 383. The trend is common to all three postseismic surveys, but is not obvious in the 1954 to 1934 elevation changes as these contain the coseismic signal. Since the deformation is observed in three postseismic surveys it is unlikely the signal is a systematic error. The observed subsidence rates between bench marks H 383 and U 47 are 2.1 mm/yr from 1967 to 1986 and 3.1 mm/yr from 1955 to 1986. The Salt Well Basin through which this section of the leveling line runs is an area of groundwater withdrawal [*Bedinger et al.* 1984]. *Seiler and Allander* [1993] report that in 1904 the depth to water along the Carson River was 1.5 m, and in 1992 the depth to water in the Fallon area was 1.5-3 m In that period Carson Lake, which the leveling line borders, has almost dried up. The Stillwater Range to the east acts as a groundwater flow barrier between Dixie Valley and the Carson Sink [*Seiler and Allander*, 1993] and thus points east of H 383 which lie on the western side of the Stillwater Range are not affected by water withdrawal.

The spatial and temporal correlation between the data and a drop in the water table suggests subsidence due to water withdrawal is occurring east of Fallon. A correction proportional to the distance between two bench marks and the time interval between the two surveys being differenced was applied to the coseismic elevation changes. The correction c was calculated as

$$c = \frac{3.2}{37.7} LdT$$

where L is the distance between two bench marks, dT is the number of years involved, 3.23 is the average subsidence rate in millimeters per year and, 37.7 is the distance over which the subsidence is occurring. This was added to the change in elevation for nine bench marks (Figure 4).

Systematic Errors in Postseismic Data

The surveys made in 1967 along Dixie 1, Dixie 2, and Dixie 3 give anomalous elevation changes when they are differenced with all other surveys which suggests the 1967 surveys contain a systematic error. Elevation changes increase proportionally to distance when the 1967 measurements along Dixie 1 are differenced with all other surveys of that route (Figure 5). The ratio of elevation change to distance is approximately 2.5 mm/km and the trend is equal and opposite when the 1967 survey is differenced with surveys made before and after it. There is no such trend when the 1955, 1973, 1978, and 1986 surveys are differenced. Along Dixie 2 there is also an equal and opposite signal when the 1967 measurements are differenced with the 1985 and 1955 surveys of that route (Figure 6). The signal remaining after the 1985 and 1955 data are differenced, however, is less than the allowed random error. The entire Dixie 3 line was measured in 1908 and 1955. Only the first and last 20 km of this line were surveyed in 1967 and only six bench marks were measured in 1950. Along

Table 3. Dates of Triangulation and Leveling Surveys Made in the Dixie Valley Area and Line Numbers (LN) of Each Survey

Dixie 1		Dixie 2		Dixie 3		Triangulation
Year	LN	Year	LN	Year	LN	Year
1934	L1960	1934	L5797	1908	USGS08	1935
1955	L15586	1955	L15588	1950	USGS50	Dec. 1953 to Jan. 1954
1967	L21083	1967	L21080	1955	L15607	July-Aug. 1954
1973	USGS73	1973	USGS73	1958	L16693	April-June 1955
1976	USGS76	1978	USGS78	1967	L21086	
1986	L24985	1985	L24887	1967	L21089	

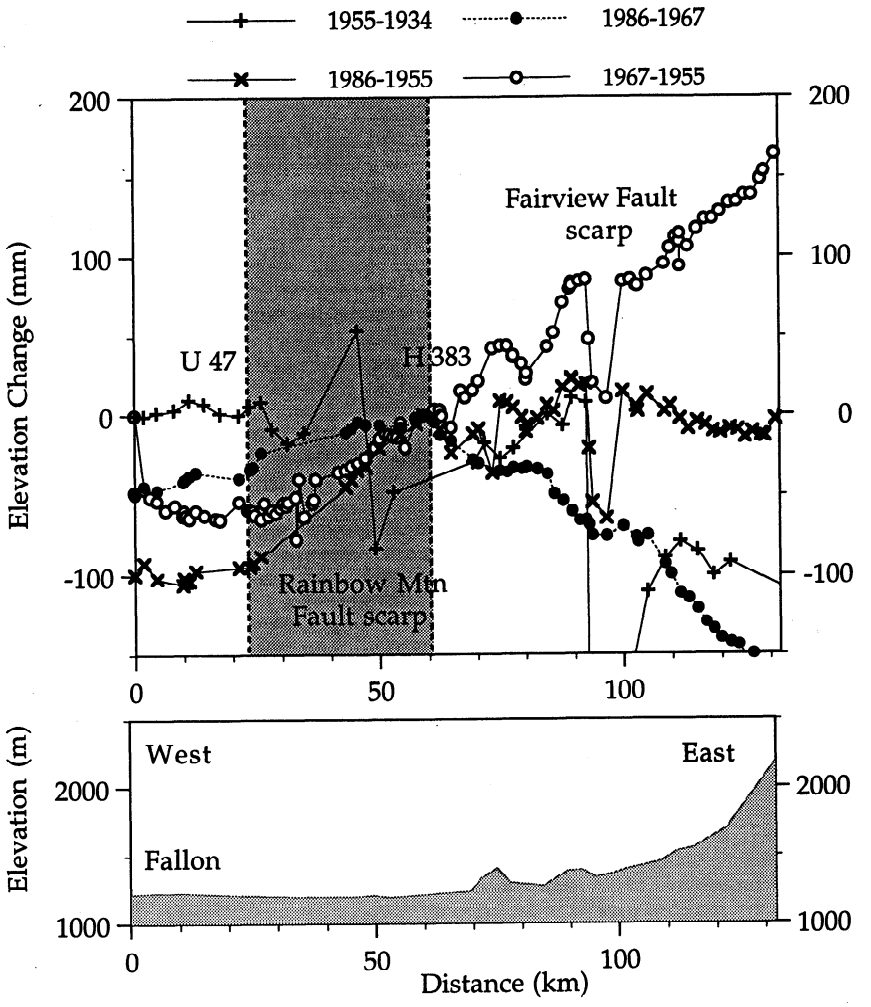

Figure 3. The elevation changes along Dixie 1 for the years 1934, 1955, 1967, and 1986. The shaded area on the elevation change between bench marks U 47 and H 383 plot indicates where subsidence due to groundwater withdrawal may be occurring. (bottom) The topography.

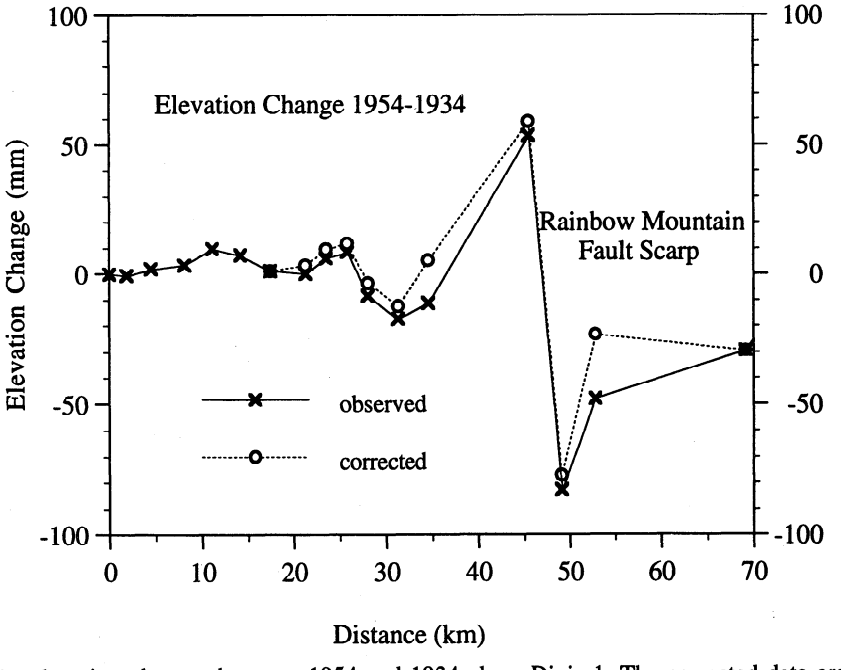

Figure 4. The elevation changes between 1954 and 1934 along Dixie 1. The corrected data are data to which a correction for water withdrawal has been applied.

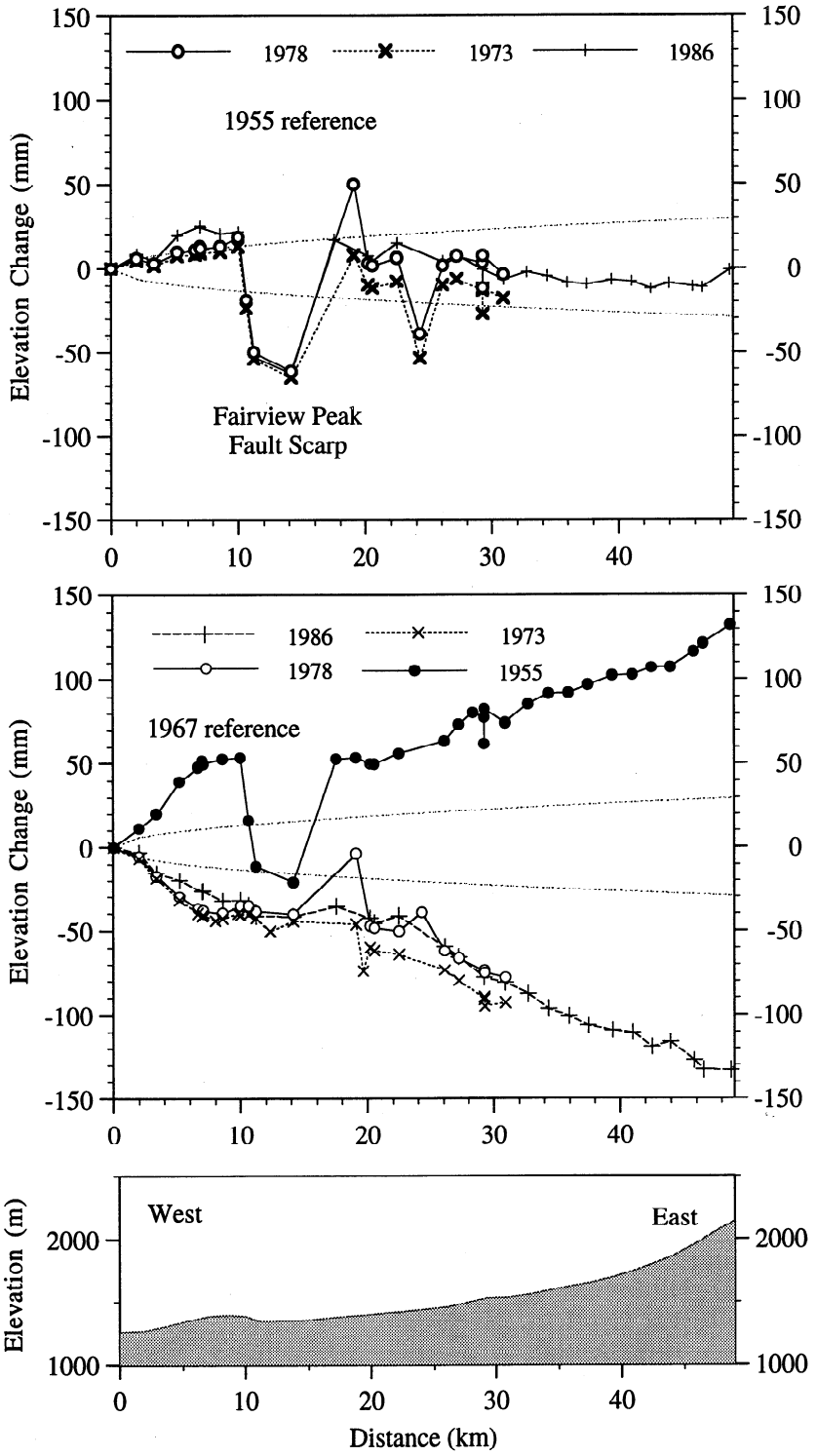

Figure 5. The elevation changes along Dixie 1, calculated from the 1955, 1967, 1973, 1978, and 1986 surveys. Dotted lines indicate the allowable accumulation of random error along the line.

the first 20 km the elevation changes between 1955 and 1967 mimic the topography (Figure 7). Along the last 20 km the measured height differences between the 1950 and 1967 surveys and between the 1950 and 1955 surveys record similar deformation (Figure 7). The elevation changes measured between the 1908 and 1967 surveys and the 1908 and 1955 surveys are also similar. Surveys of the Dixie 3 line appear to be consistent along the last 20 km, but the lack of data from this route makes it difficult to assess its consistency.

Using the method of *Stein* [1981], the elevation change per unit distance, or tilt, for each section was regressed against the gradient of the topography. Of the eight sets of elevation changes formed by differencing the 1967 surveys with other surveys, four had regression coefficients significant at the 99% confidence level and two at the 98% confidence level (Table 4). The correlation of topography with elevation change for the two data sets from Dixie 3 was not significant because there was little topographic relief. The elevation change versus

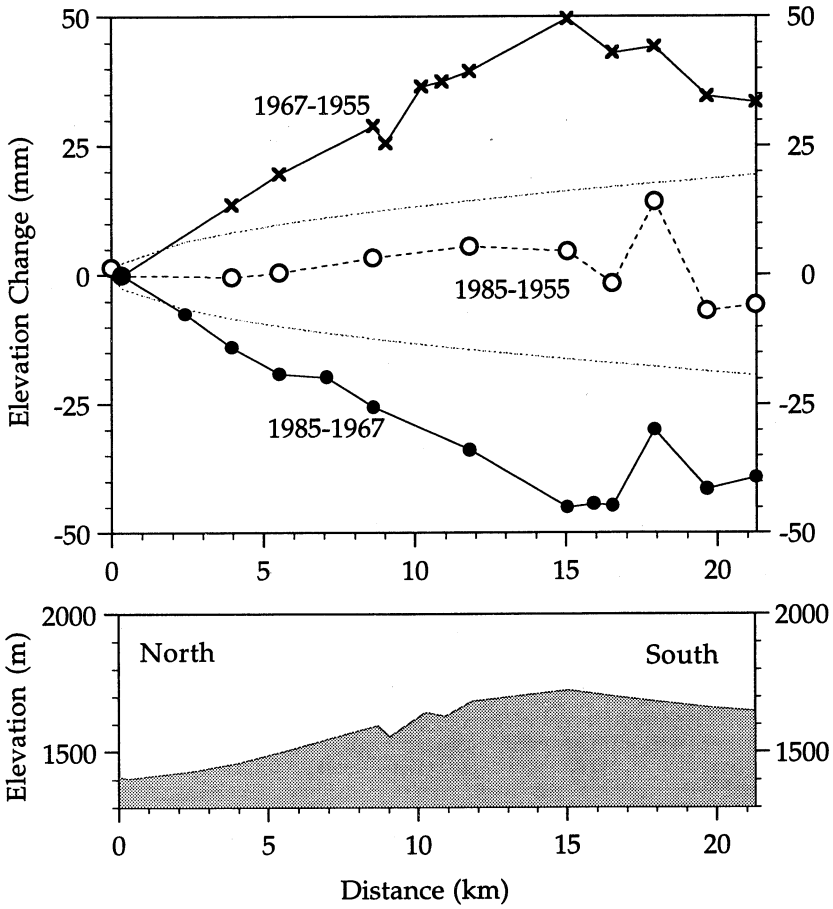

Figure 6. Postseismic elevation changes along the Dixie 2 leveling route. Dotted lines indicate the allowable accumulation of random error along the line.

topographic gradient plots for 1968-1967 and 1967-1955 are shown in Figure 8. The weighted average miscalibration of the rods is 150±30 ppm which is large compared to the typical miscalibration for rods of this period of ±30 ppm.

The three 1967 surveys along Dixie 1, Dixie 2, and Dixie 3 were made by the same crew with the same instruments and immediately after each other. The rods used in the 1967 surveys (numbered 312-347 and 312-383) where calibrated in 1965 to an accuracy of 0.05 mm. No further calibrations were made after 1965. Between 1965 and 1969, rods 312-347 and 312-38 were used in 14 surveys in New Mexico, Arizona, and Nevada and were then discarded. With the exception of the Dixie Valley survey and a survey in Gila Bend, Arizona, the rods were used mostly to cover spurs, lines of only a few kilometers long which branch off the main route (Table 5). In Gila Bend, approximately 62 km were measured using rods 312-347 and 312-383, but the route covers a region that is subsiding at a rate of 100 mm/yr due to water withdrawal. Thirty-eight sections unaffected by water withdrawal were isolated, and a rod miscalibration of -571±234 ppm was determined. Because the rods were used so infrequently after the Dixie Valley surveys, the data from the other surveys are insufficient to fix a value on the amount of rod miscalibration.

Accuracy of Leveling Data

The random error allowed to accumulate along a leveling line is expressed as, $\alpha\sqrt{L}$ where L is the length of the line in kilometers and α is the standard deviation computed from several double run sections. The uncertainty in the elevation change at each data point, δ_i, is given by

$$\delta_i^2 = \alpha_{\text{pre}}^2 + \alpha_{\text{post}}^2 \tag{1}$$

and α_{pre} and α_{post} are the standard deviations associated with the preseismic and postseismic surveys respectively. The associated uncertainty σ_i in elevation change between two bench marks i and $i+1$, which are L km apart is

$$\sigma_i = \left[\left(\frac{\delta_i + \delta_{i+1}}{2}\right)^2 L\right]^{\frac{1}{2}} \tag{2}$$

where δ_i, and δ_{i+1} are the uncertainties in the coseismic elevation changes at those points.

Three methods are used to asses the accuracy of the coseismic leveling surveys: (1) loop misclosures, (2) the difference between forward and backward runs, and (3) comparison with other surveys made under similar surveys. For each of the coseismic leveling surveys one of these methods was used to identify the accuracy of the measurements and to calculate α. The appropriate weighting could then be ascribed to each releveled section.

The misclosure of a leveling loop is the amount by which the first and last measurements of the starting bench mark differ [*Bomford*, 1971]. If the misclosure is greater than $\alpha\sqrt{L}$ then the data contain random or systematic errors or blunders. The error is distributed around the loop and a new α value

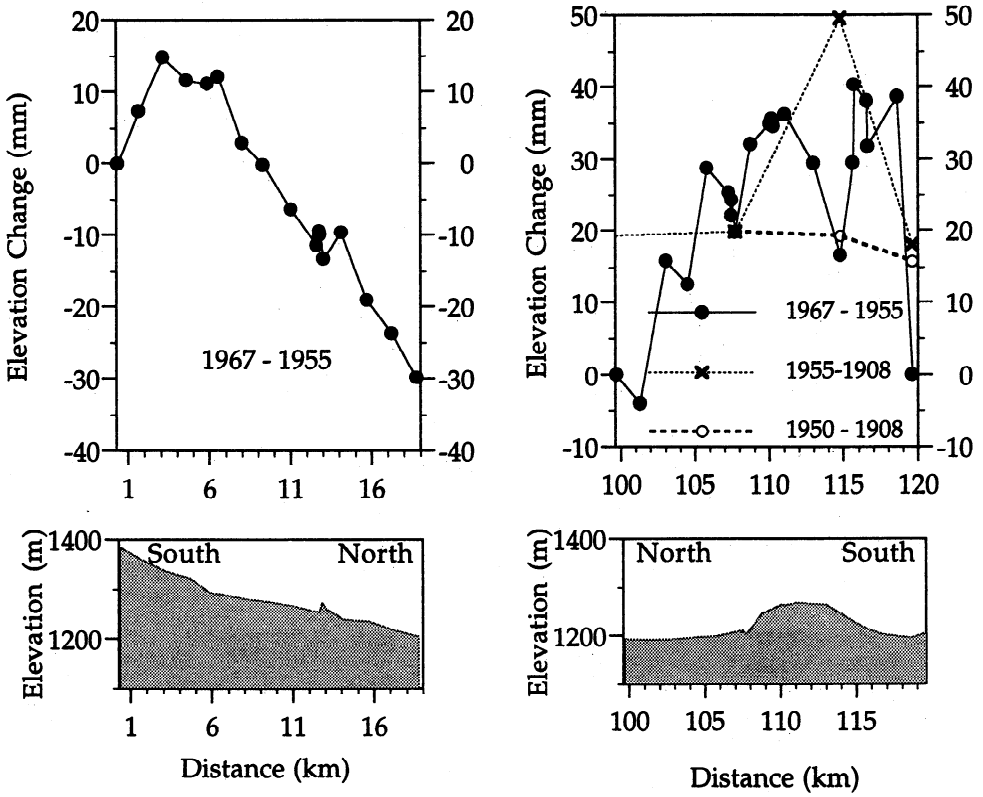

Figure 7. Elevation changes along the first and last 20 km of the Dixie 3 leveling route. The elevation changes between the first two sections on the Dixie three line do not appear related because these sections run east-west perpendicular to the rest of the line which runs north-south.

calculated using $E = \alpha\sqrt{L}$, where E is the misclosure of the loop in millimeters.

When a loop is not formed α can be calculated from the difference between the forward and backward measurements of the line. If there are no errors, then the sum of the forward observations should be equal and opposite to the backward observations. If e_i is the difference between the forward and backward measurements for section i, then α is calculated from the average misclosure of all the sections along the line, i.e.,

$$\alpha^2 = \frac{1}{4n}\sum_{i}^{i=1,n}\frac{e_i^2}{L_i} \qquad (3)$$

where n is the total number of sections and L_i is the length of each section [*Bomford,* 1971]. For leveling surveys which were not double run and did not form a closed loop, α is calculated by comparing that survey with another made under similar conditions and standards and for which α is known. If the two surveys are of similar quality then it is assumed that the α to β ratios are equal [*Marshall et al.,* 1991].

The misclosure of 1955 surveys around lines Dixie 1 and Dixie 3 is +47 mm which is almost 3 times the expected misclosure given the order of the leveling. Since no large blunders are apparent in the data, the 1955 misclosure was distributed around the loop and an α value of 3.5 mm/km$^{1/2}$ ascribed to the 1955 surveys (Table 6). The α value for

Table 4. Rod Miscalibration Coefficients (MC) and Regression Coefficients (R) Determined From Leveling Surveys Along Dixie 1, Dixie 2, and Dixie 3

Route	Years	Number of Sections	Regression Coefficient R	MC ppm	Significance, %
Dixie 1	1967-1955	50	0.474	100±26	1
Dixie 1	1978-1967	22	-0.809	-185±28	1
Dixie 1	1986-1967	42	-0.659	-89±36	1
Dixie 1	1973-1967	24	-0.859	-333±40	1
Dixie 2	1985-1967	11	-0.752	-90±25	2
Dixie 2	1967-1955	12	0.803	106±20	-
Dixie 3(i)	1967-1955	15	-0.247	-130±112	-
Dixie 3(ii)	1967-1955	17	0.303	192±140	-

No entry for the significance implies the regression coefficient is insignificant at the 5% confidence level.

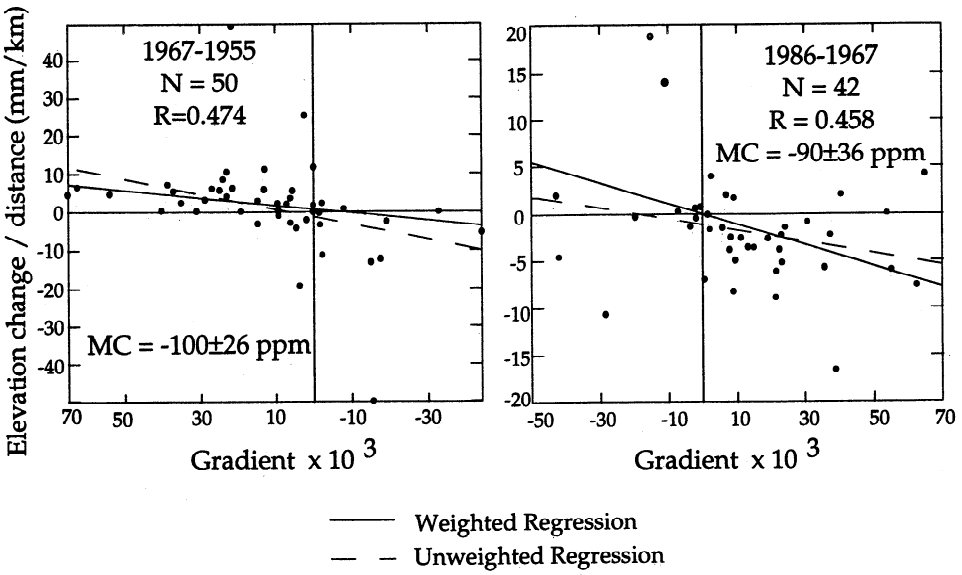

Figure 8. The elevation change per unit distance versus topographic gradient for elevation changes 1967-1955 and 1986-1967. The number of leveling sections analyzed is N, the regression coefficient R, and the rod miscalibration MC. Removal of the two outliers in the 1967-1955 plot does not reduce the correlation between tilt and gradient. These correlations should be equal in magnitude and opposite in sign if they were caused by the 1967 rod errors.

L5797, a single run survey along Dixie 2, was calculated by comparison with another 1934 survey, L1960. The α values for the other surveys were calculated using equation (3), field notebooks, and those calculated by the National Geodetic Survey for the more recent post-1980 lines (Table 6).

Triangulation Data

A triangulation survey determines the horizontal positions of points as coordinates on a plane coordinate system by measuring directional angles, azimuths, and distances between stations. A directional angle is the angle between a line joining two points with respect to an arbitrary azimuth. There are three orders of accuracy of triangulation surveying, first, second and third order. First-order surveying is the highest order of accuracy. The procedure used for triangulation surveys in the 1950s involved setting up a theodolite at one station and sighting a staff at another. Each angle was measured several times during each setup and any which deviated from the mean by more than a specified tolerance was rejected.

Three triangulation surveys made before the 1954 earthquakes and a survey made 1 year after the sequence were used to calculate the coseismic angle changes. In 1935, eight stations west of the Stillwater Range were measured as part of a survey of the primary network (Figure 9). Twenty-nine points spanning the Rainbow Mountains and Fairview Peak were surveyed between December 1953 and January 1954. Seven of the stations measured in 1935 were reoccupied. Coverage in Dixie Valley was sparse, only one point being measured in the Stillwater Range and Dixie Valley. A second survey in 1954 began 2 days after the July 6 event in the Rainbow Mountains and continued until August 23 the date of the next Rainbow Mountain earthquake. The second 1954 survey extended the network measurement east of Fairview Peak. Twelve points measured earlier that year were remeasured.

The surveys made in 1935 and 1954 provide the preseismic triangulation data. Including the 1935 survey in the preseismic data allowed greater coverage of the Rainbow Mountain fault. Measurements made west of -118.4°W in the second 1954 survey were not used to form the preseismic data set, since

Table 5. All Other Surveys Made Using Rods 312-347 and 312-383 Between 1967 and 1969

Area	Years	Leveling Lines	N	Miscalibration Coefficient, ppm	Significance
San Antonio, Texas	1967	L20946, L20943	5	325±651	0.242
Anthony, New Mexico	1967	L20952, L20955	6	540±16	0.998
Gila Bend, Arizona	1967	L21089, L21029	38	-571±234	0.506
Carrizo, New Mexico	1969	L21908	4	161±0.3	1.000

The number of releveled sections is given by N

Table 6. The α and β tolerances for Each of the Dixie Valley Leveling Surveys

Line	Year	Route	Class	α, mm	β, mm
USGS08	1908	Dixie 3	III	3.50[a]	9.0
L1960	1934	Dixie 1	I/II	1.07[b]	4.0
L5797	1934	Dixie 1	II	2.54[d]	8.4
L15586	1955	Dixie 1	I/II	4.00[c]	4.0
L15607	1955	Dixie 3	I/II	4.00[c]	4.0
L15588	1955	Dixie 2	I/II	4.00[c]	4.0
L21083	1967	Dixie 1	I/II	1.26[b]	4.0
L21086	1967	Dixie 3	I/II	0.94[b]	4.0
L21089	1967	Dixie 3	I/II	0.94[b]	4.0
L21080	1967	Dixie 2	I/II	1.00[b]	4.0

[a] Taken from USGS field notebooks.
[b] Calculated using equation (3).
[c] Calculated from misclosure of the 1955 loop.
[d] Calculated by comparing values from L1960.

they contained coseismic displacements associated with the Rainbow Mountain events. All the stations observed in 1954 were resurveyed in 1955. There are 112 coseismic observations a at 33 triangulation stations.

Quality of Triangulation Data and Assignment of Errors

The 1935 survey was a first-order survey of the primary network. The 1954 and 1955 surveys were carried out under first-order specifications for the primary network measurements and second-order for the intervening network. The standard error σ assigned to the measured angle reflects the consistency of the measurements of the angle made during one setup, the internal error, and the variation in its measurement between different setups, the external error.

The 1954 and 1955 triangulation surveys met the standard of first-order class II surveying for the primary network and second-order class I for the secondary network [*Miller,* 1967]. The standard errors normally assumed are 0.7 arc sec for first-order triangulation and 1.4 arc sec for second-order. Rather than use these conventional values (as, e.g., *Snay et al.* [1985]), the standard error of each angle measurement is used to weight the data. In this way, lower weighting could be given to data with a larger uncertainty. Misclosures within the triangles were used to reassess the quality of the data. If the misclosure was larger than the sum of the error of the three

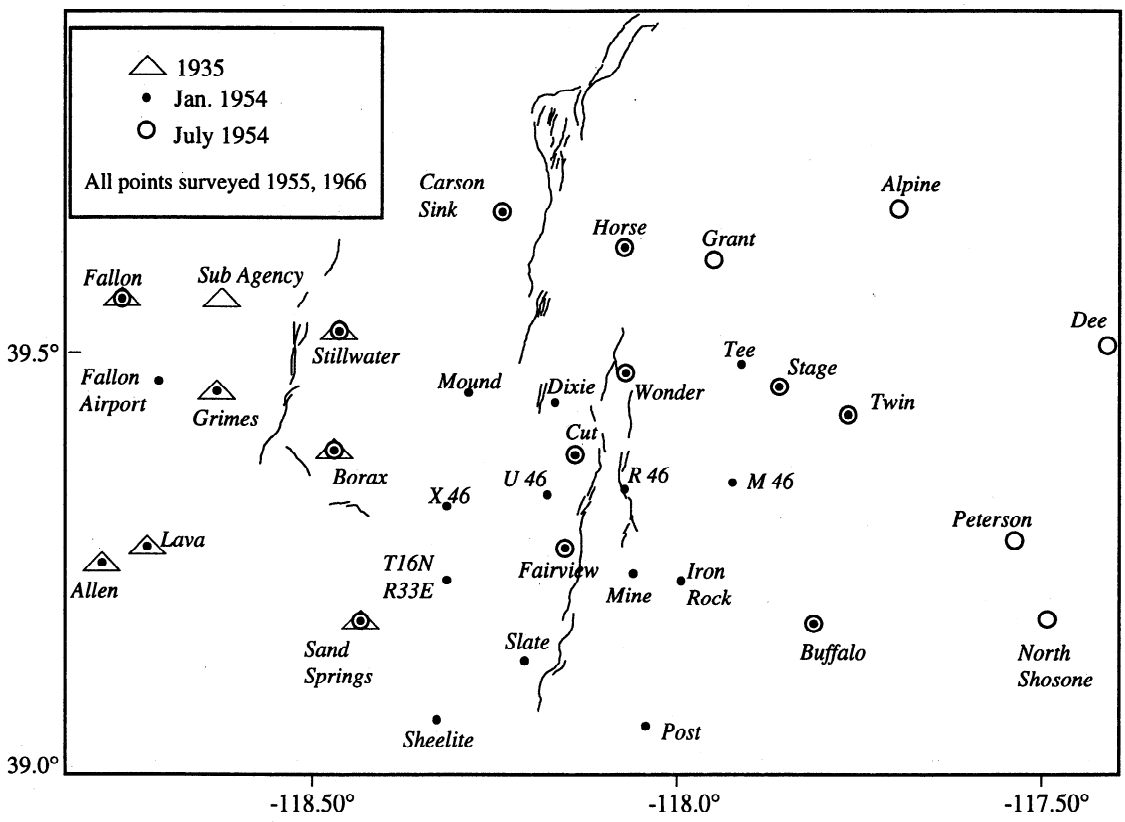

Figure 9. The triangulation network and the years each point was occupied. All points were resurveyed in 1955.

angle measurements it was distributed equally among the three measurements and assigned as the error associated with that observation. This was required for 14 of the 112 coseismic observations. The largest error assigned was 1.23 arc sec. The weighted average was calculated for any angle observed several times and the error σ assigned calculated as

$$\sigma = \left(\sum_{i=1}^{n} \frac{1}{\sigma_i^2} \right)^{\frac{-1}{2}} \tag{4}$$

where σ_i was the standard error of each measurement. The mean standard deviations for the preseismic and postseismic surveys were 0.866 and 1.05 respectively. The coseismic error $\sigma_{\text{coseismic}}$ is calculated as

$$\sigma_{\text{coseismic}} = \left(\sigma_{\text{pre}}^2 + \sigma_{\text{post}}^2 \right)^{\frac{1}{2}} \tag{5}$$

where σ_{pre} and σ_{post} are the standard errors of the preseismic and postseismic measurements, respectively.

Coseismic Modeling Method

The signal to noise ratio (S/N) of the data is expressed as

$$S/N = \left[\frac{1}{n} \sum_{i}^{n} \left(\frac{y_i}{\sigma_i} \right)^2 \right]^{\frac{-1}{2}} \tag{6}$$

where y_i are the observed values, σ_i are the uncertainties associated with the observed values, and n is the total number of observations. The S/N ratio of the leveling and triangulation data is 33 and 12, respectively. The combined data set has an S/N ratio of 22. The large signal of the leveling data is a result of some sections crossing the faults and having large elevation changes. Without these sections the leveling data have about the same influence as the triangulation data.

The fault geometries and coseismic slip were inferred by inverting the leveling and triangulation measurements to find the fault parameters, i.e., strike, dip, depth, and length, which best fit the data in the least squares sense. The goodness of fit was assessed by calculating the reduced chi-square misfit, χ_ν^2, using

$$\chi_\nu^2 = \frac{1}{\nu} \sum_{i=1}^{n} \left\{ \frac{1}{\sigma_i^2} (y_i - c_i)^2 \right\} \tag{7}$$

where c_i are the computed values and ν is the number of degrees of freedom.

The best fitting set of geometries and slip values were found using a gradient search of fault parameter space since this method can find the best fitting model by varying all the parameters simultaneously. Trial and error was used as a preliminary coarse searching method using mapped fault offsets as a starting model and a gradient search of the parameter space was then made to reduce the misfit.

In a gradient search all the fault parameters are changed simultaneously to seek the best fitting model. The coseismic observations can be represented by

$$y(\text{obs}) = a_0 + \sum_{j=1}^{n} a_j X_j \tag{8}$$

where α_j are the fault parameters and X_j are functions of the strike, dip, depth, and length. The reduced chi-square fit is assumed to be some continuous function of the fault parameters and a model which minimizes this is sought. Each parameter is incremented simultaneously by a normalized step size, thus increasing each parameter by the same amount. The value of χ^2 is recalculated; if it has been reduced, the searching continues along this gradient until χ^2 begins to increase, if there is no reduction then the process is repeated with a smaller step size [*Bevington*, 1969].

The displacement field is a nonlinear function of the fault dip, depth, strike and length. The gradient search deals with the nonlinearity of the problem but its disadvantage is that it is dependent on the starting model. Because the number of dimensions of the problem are so large there are many minimums in parameter space. However, using χ^2 as a measure of the goodness of fit enables the model fit to be quantitatively assessed.

Single Value Decomposition

Single value decomposition (SVD) was used to invert the data as this method not only estimates the fault slip gives an insight to the resolvability of slip given the data distribution [*Segall and Harris*, 1987; *Harris and Segall*, 1987; *Segall and Harris*, 1986; *Thatcher*, 1979; *Lanczos*, 1961]. The displacement at N points caused by slip on M faults can be written as

$$u = Gm \tag{9}$$

where u is a matrix of dimension Nx1 and G an NxM partial derivative matrix. The matrix m of slip values associated with each fault is one of dimension Mx1. The G matrix maps the vector in the model space to the vector in the data space and is a matrix of functions that describes the fault geometry and elastic properties of the crust. Each value m_i represents the amount of slip on a fault. Because equation (9) is mixed determined, SVD is used to invert the G matrix.

Any NxM matrix can be decomposed to

$$G = U \Lambda V^{\mathrm{T}} \tag{10}$$

where U represents an NxJ set of eigenvectors which span the data space, V represents an JxM matrix of eigenvectors which spans the model parameter space, and Λ represents a square diagonal matrix of eigenvalues. The eigenvalues are usually written in order of decreasing absolute value and the eigenvectors in U and V^T ordered accordingly. The natural generalized inverse of G is calculated as $V_p \Lambda_p^{-1} U_p^T$ were p is the number of non zero singular values [*Lanczos*, 1961; *Menke*, 1984]. The model resolution matrix is defined as $R = G^{-g} G$, and

$$G^{-g} G = \left\{ V_p \Lambda_p^{-1} U_p^T \right\} \left\{ U_p \Lambda_p V_p^T \right\} = V_p V_p^T. \tag{11}$$

The matrix R quantifies how well the slip values are resolved. The entry r_{ij} in the resolution matrix represents the resolvability of slip value i from slip value j. If the parameters are perfectly resolved, (which rarely happens), then R is the identity matrix. When all the eigenvalues are used, the SVD algorithm then becomes a weighted least squares fitting of the data; the solution is unique, independent of the starting slip values and $R = I$. SVD finds the generalized inverse of any

Table 7. Best Fitting Fault Geometries for the Rainbow Mountain, Fairview Peak, Fairview South, West Gate, Gold King and Dixie Valley Faults

Parameter	Rainbow	Fairview	Fairview south	West Gate	Gold King	Dixie
Dip	87°E	69.0°E	64.0°E	59°W	83°W	49.0°E
	31°E-35°W	64°E-75°E	36°E-80°W	49°W-73°W	70°W-71°E	39°E-57°E
Lower depth, km	14.0	8.0	8.0	8.0	5.0	5.5
	4.0-14.0*	6.5-9.5	4-12.0	5.0-11.0	2.0-6.0*	4.5-6.5
Upper depth, km	0.2	0.0	0.0	0.4	0.2	0.0
	0.0-1.0	0.0-0.5	0.0-6.0	0.0-1.0	0.0-1.5	0.0-1.0
Strike	N25°E	N4°E	N4°W	N2°E	N3°E	N8°E
	N18°E-N35°E	N2°W-N10°E	N19°W-N21°E	N13°W-N3°E	N12°W-N13°E	N4°E-N11°E
Length, km	24.9	24.16	13.2	14.8	16.2	24.3
	24-33	2-30	1.5-20.0	15-22	16.0-24.5	21-28
Latitude Npt	39.54°N	39.288°N	39.15°N	39.43°N	39.44°N	39.663°N
	39.62-39.52	39.29-39.28	39.23-39.05	39.58-39.41	39.52-39.37	39.70-39.66
Longitude Npt	-118.48°W	-118.13°W	-118.12°W	-118.062°W	-118.11°W	-118.185°W
	-118.46-118.52	-118.12-118.14	-118.07-118.16	118.06-118.14	118.09-118.15	-118.18-118.20
Latitude Spt	39.34°N	39.07°N	39.081°N	39.297°N	39.29°N	39.45°N
	39.37-39.33	39.10-39.02	39.08-39.98	39.30-39.29	39.31-39.28	39.49-39.40
Longitude Spt	-118.61°N	-118.15°W	-118.11°W	-118.068°W	-118.12°W	-118.23°W
	-118.60-118.67	-118.13-118.18	-118.07-118.12	-118.06-118.07	-118.09-118.15	-118.21-118.24

Second row for each entry is the range it can span without a 5% degradation of the model to data misfit. Npt, northern end point of fault; Sth, southern end point of fault.

[a] Constrained to this value in the optimal model.

matrix, singular or nonsingular. This method of inversion can thus be used to determine where slip is resolvable given the data distribution and where it is not. Using the resolution matrix, a process is formalized through which slip resolvability can be determined.

Typically, the model fit improves with increasing number of eigenvalues, and after a certain number of eigenvalues it is not improved by the addition of more. The problem is said to be overparameterized. An F test was used to establish how many parameters add to the complexity of the model without making a significant decrease in the misfit of observed and computed values. An eigenvalue is retained if the reduction in misfit in going from the xth eigenvalue solution to the $(x+1)$th solution had a probability of 1% or less being due to random noise. The resolution matrices formed using that number of eigenvalues indicate on which faults slip is resolvable. A solution that does not use all the eigenvalues is nonunique and dependent on the starting slip values. For a unique solution, given the fault geometries, estimates of unresolvable parameters must be found from another source and then excluded from the inversion process. The full eigenvalue solution is then found. The result is independent of the starting values.

Results

Five of the major faults were incorporated into the model: the Fairview, West Gate, Gold King, Rainbow Mountain, and Dixie Valley faults. The set of fault geometries which best fit the observations are given in Table 7 and Figure 10. The best fitting fault geometries give a reduced chi-squared fit of 1.9. Ninety percent of the data fall within the 3σ residual level and 71% within the 2σ level. The normalized residuals at each data point, r_i, are calculated as

$$r_i = \left(\frac{y_i - c_i}{\sigma_i} \right) \tag{12}$$

(Figure 11). For the triangulation points where several observations were made from one point the average residual is calculated using

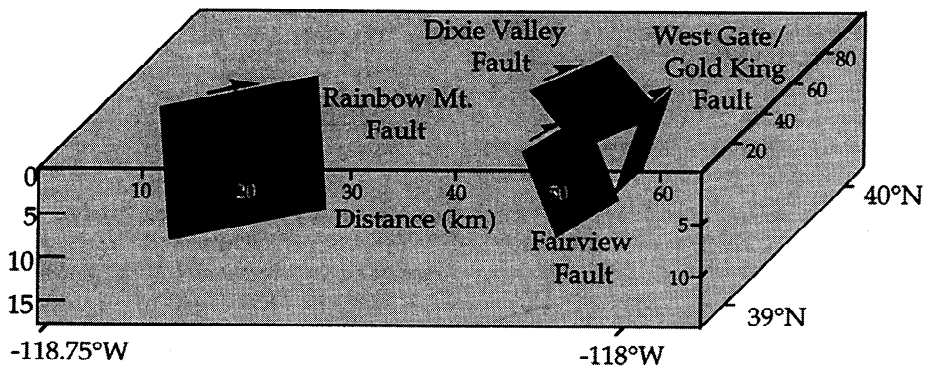

Figure 10. Best fitting fault geometry derived from the geodetic data.

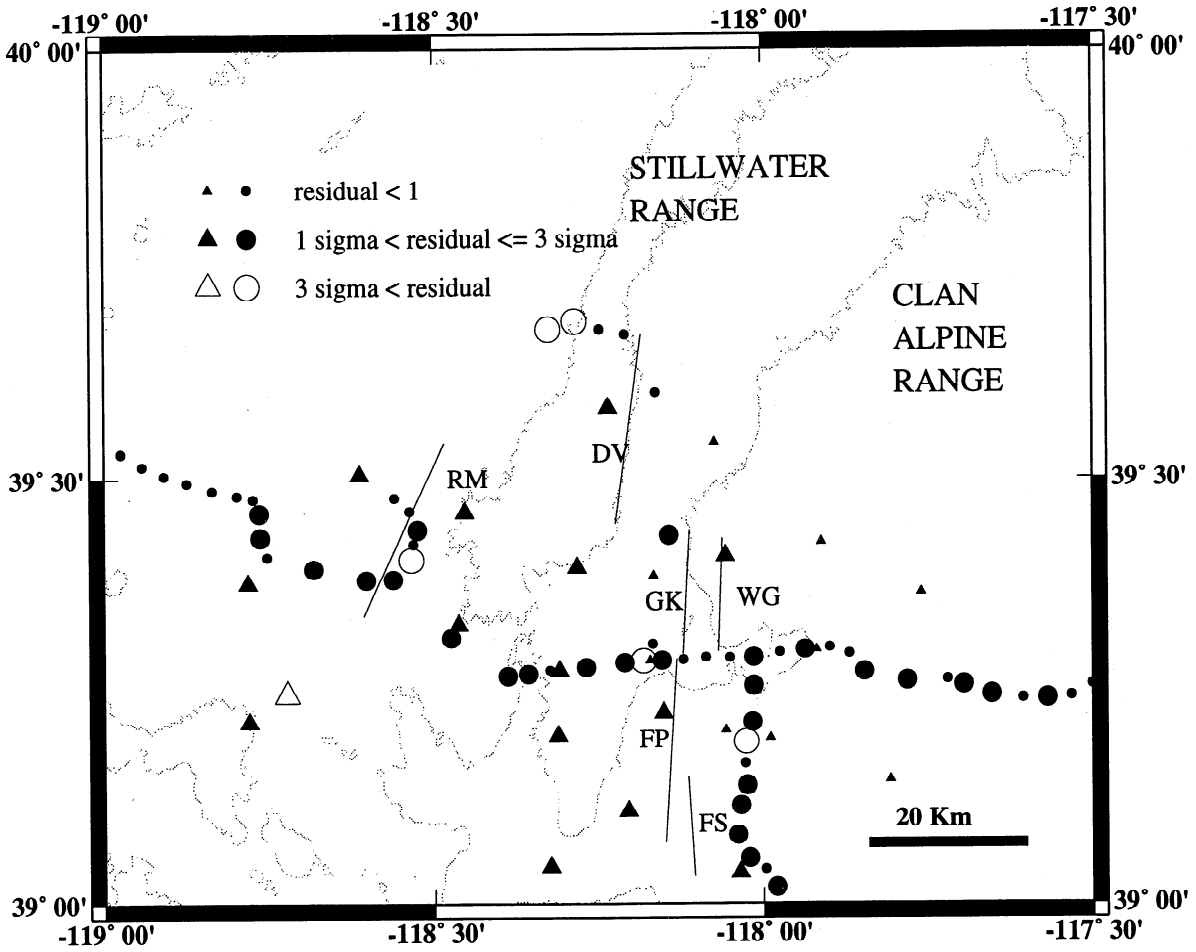

Figure 11. Normalized residuals from the inversion of the geodetic data. Each of the points representing leveling data mark the midpoint of the modeled leveling section. The positions of the modeled faults are shown by solid lines. The faults are labeled as F, Fairview; DV, Dixie Valley; WG, West Gate; GK, Gold King; RM, Rainbow Mountain, and FS, Fairview South. The 1500-m contour is shown.

$$r_i = \frac{1}{T}\sum_{i=1}^{T}\left|\left(\frac{y_i - c_i}{\sigma_i}\right)\right| \qquad (13)$$

where T is the number of observations made from that point. The influence of the leveling and triangulation data was about equal. If the triangulation data only were modeled, χ^2_ν was 1.8. If the leveling data only were modeled, χ^2_ν is 2.

The relation between the strike, dip, depth, and length of a fault and surface deformation is nonlinear ,and it is difficult to asses the trade-off between the uncertainties in each parameter. To calculate the errors in the fault geometries, each parameter was increased, while holding the others fixed until the χ^2_ν value was degraded by 5% (Table 7). The value of 5% is arbitrary, and the method does not account for the nonlinearity of the problem but serves to give an idea of how well constrained each parameter is. The best fitting geometry is used as the basic model.

Fault Geometry

The derived strike of the Fairview fault follows the surface rupture and can range from N2°W to N10°E without causing more than a 5% degradation of the model misfit (Table 7). The best fitting dip is 69°E. A second fault 5 km east of Fairview Peak was required to satisfy the leveling data along Dixie 2. We refer to this fault as Fairview South. The paucity of data across this fault, however, makes the fault geometry difficult to determine. The best fitting fault geometry for the Dixie Valley fault is one that dips 55°E, strikes N8°W and has a maximum depth of 6.5 km. The lack of data north of The Bend (Figure 1) renders the northerly extent of the fault poorly constrained. The West Gate fault is found to strike a few degrees west of north, to dip at 59°W and to have a depth of 8 km. The Gold King fault is a steeply dipping fault, though the direction of the dip, east or west, is not well constrained, ranging from 71°W to 70° E. The surface scarp dips to the west [*Slemmons,* 1957], suggesting the Gold King fault dips westward like the West Gate fault. The geodetic data place the Rainbow Mountain fault west of the mapped fault scarp, its strike and position being determined by the leveling data which run perpendicular and parallel to the scarp. The data constrain the dip poorly. The best fit was found with a dip of 87°E but the reduced chi-square was increased by 5% only outside the range 31°E to 35°W. Lower depths greater than 14 km do not reduce the misfit.

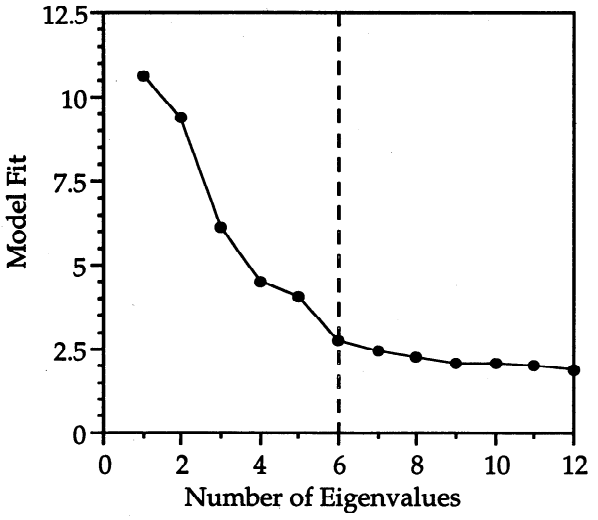

Figure 12. The model fit (reduced chi-square) versus the number of eigenvalues used in the solution. The model fit is not significantly improved after the sixth eigenvalue solution. The parameters represented by each eigenvalue are numbered 1 to 12: (1) Fairview strike slip, (2) Fairview vertical slip, (3) West Gate strike slip, (4) West Gate vertical slip, (5) Dixie Valley strike slip, (6) Dixie Valley vertical slip, (7) Gold King strike slip, (8) Gold King vertical slip, 9) Rainbow Mountain strike slip, (10) Rainbow Mountain vertical slip, (11) Fairview South strike slip, (12) Fairview South vertical slip.

Slip Estimates

The plot of model fit versus number of eigenvalues for the weighted least squares inversion solution indicates that six slip values are resolvable (Figure 12). The resolvable slip values are the vertical-slip components of the Fairview, Gold King, West Gate, Rainbow, and Dixie Valley events and the strike-slip component of the Fairview Peak earthquake. To solve for a set of slip values, which satisfy the data, given the fault geometry, the problem must be reparameterized and a priori information introduced. Slip on the West Gate and Gold King faults could not be distinguished because the faults are only 3 to 4 km apart. Therefore they were combined, and the best fitting position of the combined fault was determined from the triangulation data. The model then consisted of five faults. To show where slip on the faults is best resolved, the resolution was calculated on 1- to 2-km sections along each major fault (Figure 13). Along the Fairview Peak fault both strike-slip and vertical-slip motions are well resolved where the leveling lines cross the fault (Figure 13a). There is a small improvement at 17 km where a triangulation station lies close

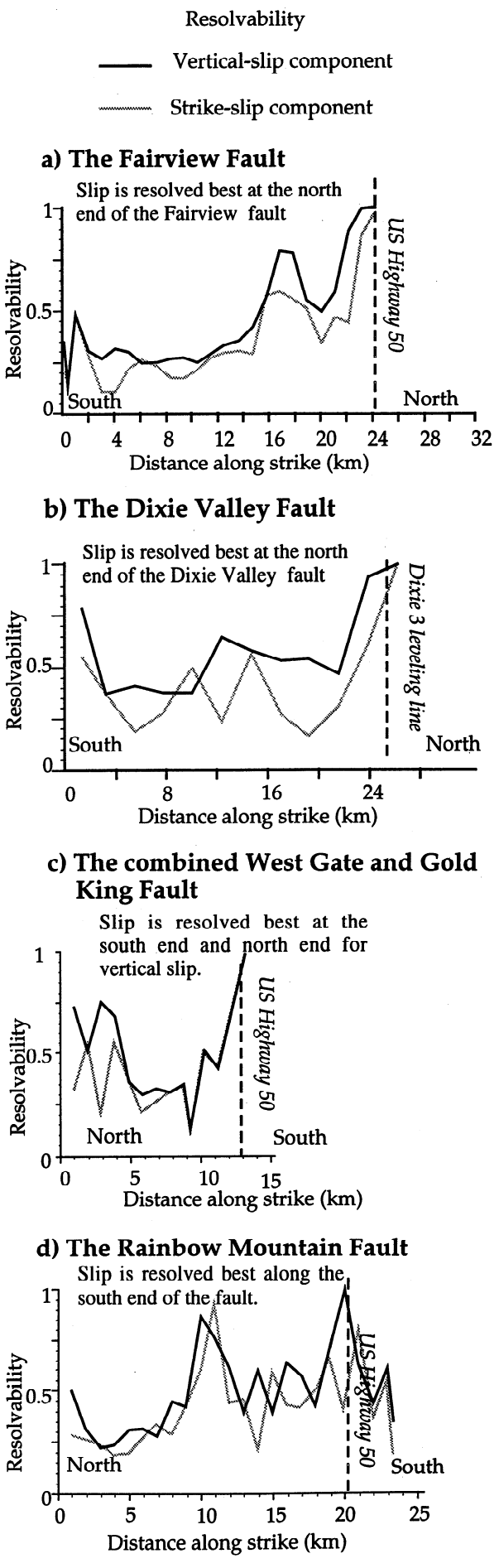

Figure 13. Resolution of slip along the major faults at 1- to 2-km points along the fault. The value plotted is the diagonal of the resolution matrix calculated at the eigenvalue solution where the model fit was no longer improved by using further eigenvalues in the solution. The solid line represents resolution of the vertical-slip component, and the shaded line represents the resolution of the strike-slip component. (a) Fairview Peak fault, (b) the Dixie Valley fault (c) the combined West Gate fault and Gold King fault, and (d) the Rainbow Mountain fault. Dashed lines show where leveling routes cross the faults (Dixie 1 lies along U.S. Highway 50).

to the fault. Similarly, slip is well resolved along the Dixie Valley fault where the leveling route crosses the fault scarp (Figure 13b). South of this point the lack of data renders slip unresolvable. Along the combined West Gate and Gold King fault, resolution is best at the southern end of the fault where the geodetic network is strong (Figure 13c). Slip is best resolved along the southern half of the Rainbow Mountain fault again, where the leveling line runs across and parallel to the fault (Figure 13d).

To attain a weighted least squares unique solution the slip values held fixed and not inverted for were the following: vertical-slip motion on the combined West Gate/Gold King fault, strike-slip motion on the Fairview South fault, and strike-slip motion on the Dixie Valley fault. The horizontal displacements of about 20 cm on small scarps mapped by *Slemmons* [1957] in the Bell Flat area were used as an a priori estimate of the strike-slip motion on the Fairview South fault. An estimate of the vertical-slip motion on the combined West Gate/Gold King fault was obtained by summing the two vertical-slip values determined from the weighted least squares solution for the separate West Gate and Gold King faults since these values were resolvable. The mapped horizontal offset of zero along the Dixie Valley fault was used as an a priori estimate for that parameter.

The shear strain across the Fairview, Fairview South, West Gate/Gold King, and Dixie Valley faults was calculated from the triangulation data using Frank's method and used to assess the assumption of zero horizontal slip on the Dixie Valley fault [*Frank,* 1966; *Savage and Burford,* 1970]. The shear strain across these four faults, calculated using Frank's method was 38.7 ppm oriented at N14°W. Over a zone 59 km long this represents a total strike-slip motion of 2.22 m. The strike-slip motion found assuming pure normal motion on the Dixie Valley fault was 3.38 m on the Fairview fault and 3.29 m on the combined West Gate/Gold King fault. The weighted average slip (the fault length was used as a weighting), calculated using these values, is 1.7 m which is 23% less than Frank's method suggests. The deficit may be caused by underestimating the slip on the Dixie Valley fault. Calculating the horizontal slip from the 2.22 m of strike-slip motion determined from Frank's method results in 1.58 m of horizontal slip on the Dixie Valley fault.

Holding the amount of horizontal slip on the Dixie Valley fault at zero or 1.58 m makes no significant difference to the overall fit when the data are inverted, and there is little difference to slip values estimated on the other faults. This is a result of the small number of observations made across the fault and the inability of the network to illuminate slip along most of the Dixie Valley fault (Figure 13b). Using Frank's method does not circumvent the paucity of data, but it does give an estimate of strike-slip motion from the triangulation data which are independent of fault geometries and assumed slip vectors. The final slip estimates calculated using this value are given in Table 8.

The moments of the Dixie Valley, Rainbow Mountain, and Fairview Peak earthquakes were calculated using $M_0 = \mu w L \tilde{s}$, where μ is the shear modulus (3×10^{11} dyne-cm^2), w is the width of the fault, L is the length and $\tilde{s}$ is the slip determined geodetically (Table 8). The moment calculated for the Fairview Peak event includes those of the West Gate/Gold King and Fairview South events. The estimates for the Fairview Peak and Rainbow Mountain earthquakes are similar to those estimated from teleseismic analysis [*Doser,* 1986] but the Dixie Valley event is almost twice as large. The teleseismic estimate of the Dixie Valley earthquake, however, suffers from being in the coda of the Fairview Peak event. The moments found from the geodetic data are similar to the geologic moments calculated using the average offsets observed along the surface rupture (Table 8).

The errors in the fault geometry and in the slip values reflect the uncertainty of the observations. These uncertainties arise from the accuracy of the measurements and have been accounted for in the above analysis. Each coseismic elevation or angle change has been appropriately weighted given the accuracy of the survey involved and the misclosure of leveling loops or triangles. The range of errors in the fault geometries are also effected by uncertainty in the position of the faults. We have reduced this effect by searching for the position of the faults simultaneously with the dip and depths of the fault in a gradient search of the parameter space. The factors which have greatest impact on the range of the errors involved however, are the assumptions of uniform slip on rectangular dislocations, and weaknesses in the geodetic network. The triangulation data give little resolvability of the strike-slip

Table 8. Final Coseismic Displacements and Seismic Moments Determined From a Weighted Least Squares Inversion of the Data

Fault	Displacement, m		Moment, $\times 10^{18}$ Nm		
	Strike slip	Vertical slip	Seismic	Geologic	Geodetic
Rainbow Mountain	0.91±0.06	0.21±0.08	9.9	6.4	9.8±4
Fairview	3.37±0.03	1.82±0.02	53.0[a]	114.0 (40)[a]	46.3±2.4[a]
Fairview South	0.20[b]	1.15±0.05			
West Gate/Gold King	3.35±0.06	1.60[b]			
Dixie Valley	1.58[b]	3.58±0.20	9.8	90.0 (28)	22.4±1 (18)

The moments of the Dixie Valley earthquake assuming zero right-lateral slip is given in parentheses for comparison. The geologic moment of all the events except the Rainbow Mountain earthquakes are from Table 1 of *Caskey et al.* [1996], and the total moment given for Fairview Peak event includes that of the West Gate, Gold King, and Louderback Mountains earthquakes. The moments derived using the maximum offsets are given and the numbers in parentheses represent that calculated using the average offsets. The moment of the Rainbow Mountain earthquake is derived from the measurements of *Tocher* [1956]. The seismicity derived moments are from body wave modeling [*Doser,* 1986].

[a] Total moment of the Fairview Peak, West Gate/Gold King and Fairview South events.

[b] Constrained to this value.

motion of the other faults because the angle changes involved are small at distances greater than 10 km from the ruptures. The paucity of data in Dixie Valley and across the Dixie Valley fault makes it difficult to constrain the coseismic slip of the Dixie Valley earthquake.

Discussion

The leveling data constraining the coseismic deformation in the Dixie Valley area were contaminated by rod miscalibration errors and subsidence due to groundwater withdrawal. The isolation of the rod miscalibration error in the 1967 data and the correction of subsidence allow the data to be used to invert for source models of the 1954 earthquakes. The correction for water withdrawal is applied to the leveling data constraining the deformation associated with the Rainbow Mountain earthquakes. It is unlikely that the anomalous trends measured in the 1967 surveys are tectonic effects. Deformation caused by postseismic relaxation would be centered on the fault scarp [*Melosh and Raefsky*, 1983], but the trend observed along the Dixie 1 line is a tilt down-to-the-west before 1967 and down-to-the-east afterward.

The geodetic data that constrain the coseismic deformation are fit well with 50° to 80° dipping planar faults extending to depths of 5 to 14 km, geometries similar to those determined for other Basin and Range faults. The M=6.9 1915 Pleasant Valley earthquake, which occurred 100 km from the Dixie Valley epicenter struck on a 44°±8° dipping fault at a depth of 9±5 km [*Doser*, 1988]. The M=6.7 1932 Cedar Mountain event (45 km south of Dixie Valley) generated on a 72°±7° dipping fault at 14±2 km depth and the M=6.1 1930 Excelsior Mountain earthquake occurred on a fault dipping 40°±8° at a depth of 14±10 km [*Doser*, 1988]. Geodetic analysis of the M=7.3 1959 Hegben Lake, Montana, and the M=6.9 1983 Borah Peak, Idaho, earthquakes indicated slip extending to depths of 7 to 14 km and faults which dipped 45° to 50° [*Barrientos et al.* 1987]. The reasonable fit of the data to the model tends to support the seismic evidence of *Doser* [1986] that the events generated on planar faults.

The geometry derived from the leveling and triangulation data for the Fairview fault is similar to that determined by forward modeling of the triangulation data by *Savage and Hastie* [1969]. The only difference is the smaller length of the fault, a result of the inclusion of the West Gate and Gold King faults in this model. The dip of the fault is similar to that determined by *Snay et al.* [1985] using triangulation data for a deep Fairview fault buried below a shallower one (Table 1). The derived geometry of the Dixie Valley fault is also similar to that determined by *Snay et al.* [1985] given the large uncertainties and consistent with the focal mechanism except for the focal depth which is estimated to be 12±3 km [*Doser*, 1986]. A reasonable fault geometry for the Rainbow Mountain fault is derived. The fault geometry is consistent with source parameters determined from body wave modeling and the fault is not as long as that determined by *Snay et al.* [1985]. The difference may be a result of constraining motion at the extremity of the network in that study.

Along the Fairview fault trace the maximum observed vertical offsets of 3.8 m are twice that of the geodetically determined value (Figure 14a) [*Caskey et al.*, 1996]. The coseismic deformation is best constrained where Dixie 1 crosses the Fairview fault and by the leveling data. At that point the vertical surface offsets are up to 1.0 m. Thus, the geodetic result seems to be influenced by the leveling measurements across this part of the fault. The geodetically determined right-lateral motion is 3.36 m and larger than the maximum fault offset observed at the Earth's surface (Figure 14a). Along the Rainbow Mountain fault the geodetically derived slip values are close to that observed at the surface (Tables 2 and 8).

Since the West Gate and Gold King faults were modeled as one, fault it is not possible to make a direct comparison between the slip observed along the ruptures and the geodetically determined slip. The right-lateral offset determined geodetically along the combined fault is 3.3 m. No horizontal slip is observed at the surface along the Gold King fault, while up to 1.2 m of right-lateral offset is measured at two locations along the West Gate fault (Figures 14b and 14c). Recent mapping of the east side of Dixie Valley has revealed a previously unknown fault, the Louderback Mountains fault, which lies subparallel to the West Gate and Gold King faults [*Caskey et al.* 1996]. The surface trace of the Louderback Mountains fault is 14 km long and begins 100 m north of the Fairview fault [*Caskey et al.* 1996]. It is only 1.5 km west of the Gold King fault at the southern end of the Gold King fault [*Caskey et al.* 1996]. As much as 2 m of right-lateral slip may have occurred on the Louderback Mountains fault in the 1954 sequence [*Caskey et al.*, 1996]. If the maximum right lateral displacement measured along the Louderback Mountains fault (2 m) is added to that measured along the West Gate and Gold King faults, then the geodetically derived and observed slip values are similar. Remodeling of the data including the Louderback Mountains fault did not reduce the misfit by a significant amount, probably because the motion on the fault had been accommodated by increasing the amount of slip on the West Gate and Gold King fault.

Along the Dixie Valley fault the geodetically determined vertical slip is larger than the maximum observed surface offset (Figure 14d). If, however, the vertical slip on the piedmont fault is included in the surface offsets associated with this earthquake then the discrepancy between the observed and calculated offsets are reduced. Given the weakness of the triangulation network in Dixie Valley, it is difficult to determine the amount of strike-slip motion on the Dixie Valley fault. Right-lateral motion on the Dixie Valley fault may range from zero, as observed at the surface rupture [*Caskey et al.*, 1996], to 1.58 m as determined using Franks' method. Using either slip value does not significantly change the model to data fit, again an indication of the poor resolution along the fault. If 1.58 m of right-lateral slip did occur, then it did so at depth. Source parameters of the Pleasant Valley earthquake derived from body wave modeling suggest 3.3 m of vertical and 1.6 m of horizontal slip occurred on that fault, compared to vertical surface offsets of 2 m and small amounts of horizontal displacement [*Doser*, 1988]. It is also possible that some of the observed motion on the Louderback Mountains fault is being assigned to the Dixie Valley fault.

These results show that the coseismic slip determined geodetically are either similar to or greater than the maximum offsets observed at the surface. The implication is that greater slip may occur at depth than is observed along the surface rupture. The only exception is the vertical-slip motion determined on the Fairview fault which is much smaller than observed at the surface. A mismatch between surface offsets and geodetically derived slip has been found for other Basin

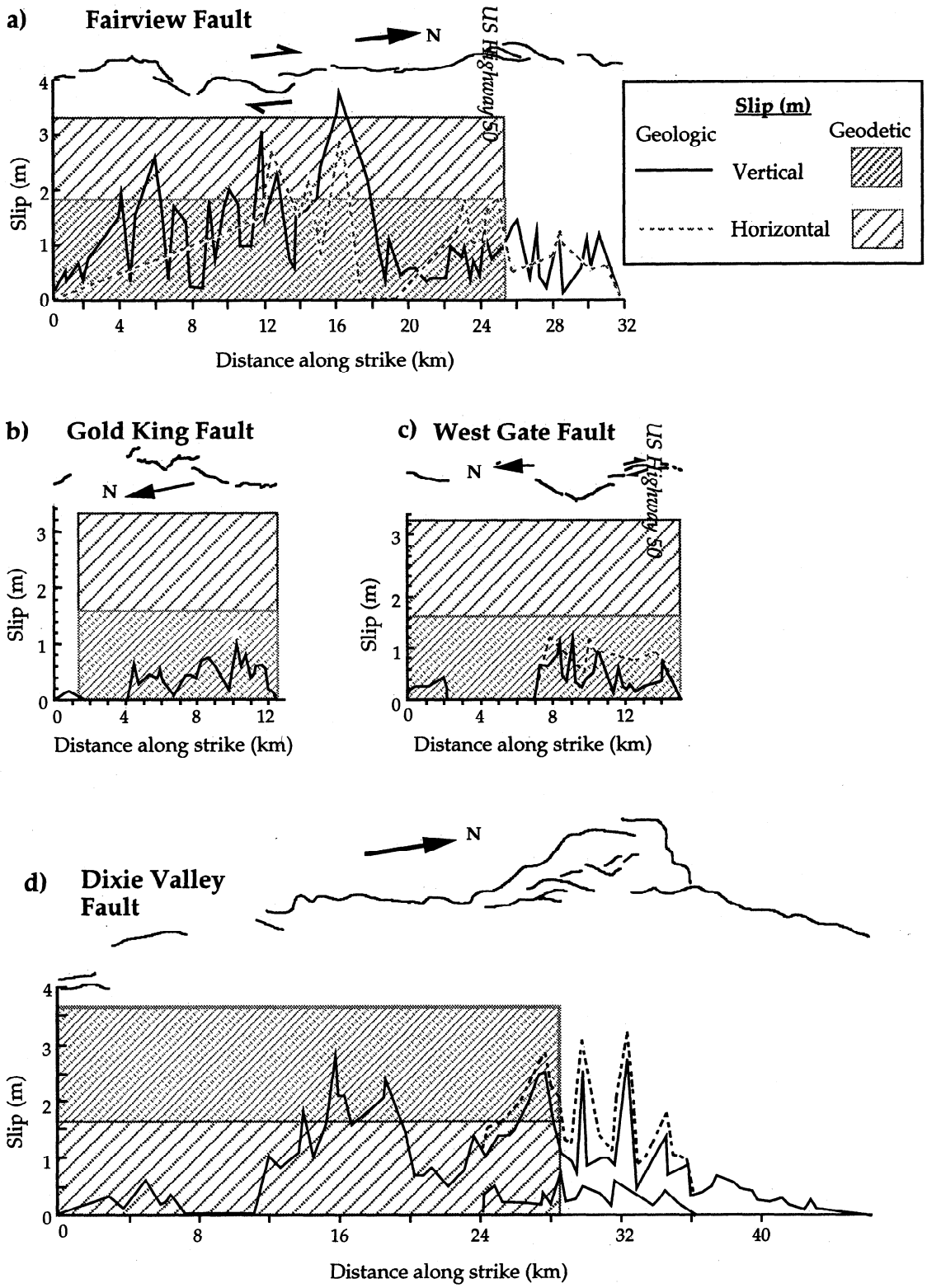

Figure 14. The mapped surface offsets and the geodetically derived slip values with distance along the (a) Fairview Peak fault, (b) West Gate fault, (c) Gold King fault and (d) the Dixie Valley fault (adapted from *Caskey et al.* [1996]). The fault scarp surface traces are shown above each plot. The mapped vertical ground separation is shown as a solid line while the mapped horizontal slip is indicated by a gray dashed line. In Figure 14d the sum of the vertical slip on the Dixie Valley fault and the piedmont fault is shown as a dashed line.

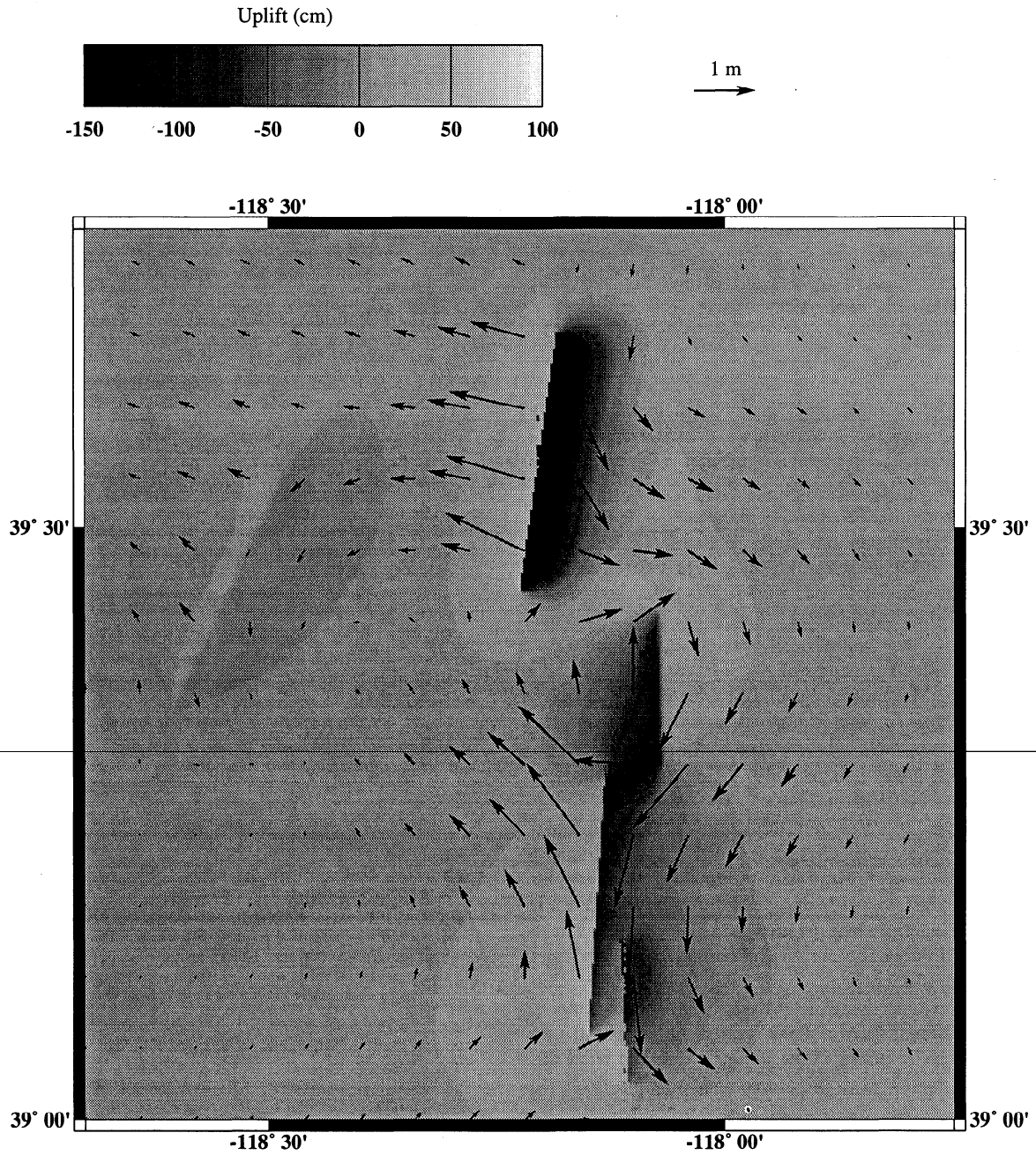

Figure 15. The coseismic horizontal deformation field, calculated using the slip vectors determined from the data inversion and given in Table 8. A value of 1.58 m was used for the right-lateral strike-slip component on the Dixie Valley fault.

and Range earthquakes. The calculated average vertical slip for the Borah Peak earthquake (2.1 m) was larger than the average surface offsets but was close to the observed maximum offset of ~2.4 m [*Barrientos et al.,* 1987]. The modeled vertical slip for the Hegben lake earthquake (7-8 m) was more than twice than the average slip observed at the surface (3 m) [*Barrientos et al.,* 1987]. If surface offsets are an underestimation of slip at depth, recurrence intervals calculated from the amount of coseismic slip divided by the long-term average rate of slip may be underestimated if based on the surface slip.

The tendency to overestimate slip in a geodetic analysis such as this may be a result of the assumption of uniform slip on a rectangular fault plane. This assumption probably leads to an underestimation of the true depth of the fault since slip probably gradually decreases to zero. Hence slip estimates may be overestimated to compensate for the underestimation of fault depth. However, while the lower depth of the fault ,may be underestimated at some places along the fault it is also likely to be overestimated at others. Thus the slip values determined are actually an average of the coseismic slip over the fault plane.

The orientation of the slip vectors associated with the 1954 earthquakes are N12°W to N13°E for the Fairview and West Gate/Gold King events. The slip vector for the Dixie Valley earthquake ranges from N72°W, assuming no right-lateral slip,

to N43°W assuming 1.58 m of right-lateral slip. Thus the extensional deformation within Dixie Valley rotated from a NNW-SSE orientation in the southern part of the valley to a NW-SE orientation to the north (Figure 15). The slip vector associated with the Fairview Peak and West Gate/Gold King events are consistent with Very Long Baseline Interferometry (VLBI) measurements across the western Basin and Range province which indicates extension oriented at N16°W±8°W [*Dixon et al.,* 1995]. Also, Global Positioning System (GPS) measurements within the Central Nevada Seismic Zone show that the zone may be represented as a right-lateral shear zone trending N15°W [*Savage et al.,* 1995].

Conclusions

Source models for the major earthquakes involved in the 1954 Rainbow Mountain-Fairview Peak-Dixie Valley earthquakes have been determined through an inversion of both vertical and horizontal geodetic data which constrain the coseismic deformation. Analyses of 32 years of postseismic leveling measurements in the Dixie Valley area show that inconsistencies in the postseismic data have two sources, a miscalibration of the 1967 rods of 150±30 ppm, and water withdrawal in the Fallon area. The corrected coseismic deformation fits the data well assuming planar fault geometries that extend to depths of 8 to 14 km.

Slip is resolved best where leveling routes cross the faults, and the ability to resolve slip declines sharply with distance from these points. The ratio of strike-slip to vertical-slip motion for the 1954 sequence shows it was not simply a sequence of extensional normal faulting earthquakes. Up to 3.6 m of right-lateral slip is found on the Fairview fault and a total of about 3.5 m slip is found on the faults which border the east side of Dixie Valley. A significant component of strike-slip motion was found in the coseismic geodetic measurements for all the events. Generally, the geodetically derived slip values are similar to or greater than the maximum displacements observed at the surface. When displacements on the Louderback Mountains fault are included with displacements on the West Gate and Gold King faults the observed and calculated offsets are similar. The moments derived from the geodetically inferred slip are consistent to the geologic moments derived using the average surface slip values. The geodetic data suggest that the Fairview Peak and the Dixie Valley earthquakes may have had greater strike-slip motion at depth than was observed at the surface.

Acknowledgments. The Dixie Valley leveling and triangulation data were supplied by the National Geodetic Survey. Emery Balazs and Sanford Holdhal of the NGS provided details of the leveling rod calibrations and surveys. We thank Mike Lisowski for discussions on using triangulation data, Wayne Thatcher for letting us use his matrix inversion software, and Gillian R. Foulger for her reviews of this work which formed part of K. Hodgkinson's Ph.D. thesis. We also thank the reviewers for useful suggestions and comments. In particular, we wish to thank John Caskey for giving us his surface slip data to compare our results to. The paper has been greatly improved by his input and careful review.

References

Barrientos, S.E., R.S. Stein, and S.N. Ward, Comparison of the 1959 Hegben Lake, Montana, and the 1983 Borah Peak, Idaho, earthquakes from geodetic observations, *Bull. Seismol. Soc. Am., 77,* 784-808, 1987.

Bedinger, M. S., J.R. Harrill, and J.M. Thomas, Maps showing groundwater units and uithdrawal, Basin and Range Province, Nevada, *U.S. Geological Survey, Water-Resources Investigation, 83-4119-A,* 1984.

Bell, J.W. and T. Katzer, Timing of late Quaternary faulting in the 1954 Dixie Valley earthquake area, central Nevada, *Geology, 18,* 622-625, 1991.

Bevington, P.R., *Data Reduction and Error Analysis for the Physical Sciences,* 336 pp., McGraw-Hill, New York, 1969.

Bomford, G., *Geodesy,* Oxford Univ. Press, New York, 1971.

Caskey, S.J., S.G. Wesnousky, P. Zhang, and D. B. Slemmons, Surface faulting of the 1954 Fairview Peak (*Ms*=7.2) and Dixie Valley (*Ms*=6.9) earthquakes, central Nevada, *Bull. Seismol. Soc. Am.,86, 761-787,* 1996.

Dixon, T.H., S. Robaudo, J. Lee, and M.C. Reheis, Constraints on present day Basin and Range deformation from space geodesy, *Tectonics, 14,* 755-772, 1995.

Doser, D.I., Earthquake processes in the Rainbow Mountain-Fairview Peak-Dixie Valley, Nevada region 1954-1959, *J. Geophys. Res., 91,* 12,572-12,586, 1986.

Doser, D.I., Source parameters of earthquakes in the Nevada Seismic Zone, 1915-1943, *J. Geophys. Res., 93,* 15,001-15,015, 1988.

Frank, F.C., Deduction of earth strains from survey data, *Bull. Seismol. Soc. Am., 56,* 35-42, 1966.

Harris, R.A., and P. Segall, Detection of a locked zone at depth on the Parkfield segment of the San Andreas fault, *J. Geophys. Res. 92,* 7,945-7,962, 1987.

Lanczos, C., *Linear Differential Operators,* 564 pp, D. Van Nostrand, Princeton, N.J., 1961.

Marshall, G. A., R. S. Stein, and W. Thatcher, Faulting geometry and slip from coseismic elevation changes: The 18 October 1989, Loma Prieta, California, earthquake, *Bull. Seismol. Soc. Am., 81,* 1660-1693, 1991.

Melosh, J., and A. Raefsky, Anelastic response to a dip-slip earthquake, *J. Geophys. Res., 88,* 515-526, 1983.

Menke, W., *Geophysical Data Analysis: Discrete Inverse Theory,* 260 pp, Academic Press Inc., San Deigo, Calif., 1984.

Miller, R.W., Vicinity of Fallon, Nevada, Earthquake movement study in the vicinity of Fallon, Nevada, *Rep. 564,* U.S. Coast and Geod. Surv., Rockville, Maryland, 1967.

Romney, C., Seismic waves from the Dixie Valley-Fairview Peak earthquakes, *Bull. Seismol. Soc. Am., 47,* 301-309, 1957.

Savage, J.C., and R.O. Burford, Accumulation of tectonic strain in California, *Bull. Seismol. Soc. Am., 60,* 1877-1896, 1970.

Savage, J.C., and J.P. Church, Evidence for post earthquake slip in the Fairview Peak, Dixie Valley, and Rainbow Mountain fault areas of Nevada, *Bull. Seismol. Soc. Am., 64,* 687-698, 1974.

Savage, J. C., and L.M. Hastie, A dislocation model for the Fairview Peak, Nevada, earthquake, *Bull. Seismol. Soc. Amer., 59,* 1937-1948, 1969.

Savage, J.C., M. Lisowski., J.L. Svarc, and W.K. Gross, Strain accumulation across the central Nevada seismic zone, 1973-1994, *J. Geophys. Res., 100,* 20,257-20,269, 1995.

Segall, P., and R.A. Harris, Slip deficit on the Parkfield, California section of the San Andreas fault as revealed by inversion of geodetic data, *Science, 233,* 1404-1413, 1986.

Segall, P., and R.A. Harris, Earthquake deformation cycle on the San Andreas fault near Parkfield, California, *J. Geophys. Res., 92,* 10,511-10,525, 1987.

Seiler, R.L., and K.K. Allander, Water-level changes and directions of ground-water flow in the shallow aquifer, Fallon area, Churchill County, Nevada, *U.S. Geol. Surv. Water Resour. Invest. 93-4118,* 1993.

Slemmons, D.B., Geological effects of the Dixie Valley-Fairview Peak, Nevada, earthquakes of December 16, 1954, *Bull. Seismol. Soc. Am., 47,* 353-376, 1957.

Snay R., M.W. Cline, and E.L. Timmerman, Dislocation models for the 1954 earthquake sequence in Nevada, *U.S. Geol. Surv. Open File Rep.* 85-290, 1985.

Stein, R.S., Discrimination of tectonic displacement from slope-dependent errors in geodetic leveling from southern California, 1953-1979, in *Earthquake Prediction: An International Review, Maurice Ewing Ser. Vol. 4,* edited by D. W. Simpson and P. G. Richards, pp 441-456, AGU, 1981.

Thatcher, W., Systematic inversion of geodetic data in Central California, *J. Geophys. Res., 84,* 2283-2295, 1979.

Tocher, D., Geologic setting of the Fallon-Stillwater earthquakes of 1954, *Bull. Seismol. Soc. Am.*, 10-14, 1956,

Wallace, R.E., Patterns and timing of Late Quaternary faulting in the Great Basin and Range Province and relation to some regional tectonic features, *J. Geophys. Res.*, *89*, 5763-5769, 1984.

Whitten, C.A., Geodetic measurements in the Dixie Valley area, *Bull. Seismol. Soc. Am.*, *47*, 321-325, 1957.

K. M. Hodgkinson and R. S. Stein, U.S. Geological Survey, MS 977, 345 Middlefield Road, Menlo Park, CA 94025. (e-mail: kathleen @usgs.gov; rstein@usgs.gov)

G. Marshall, Trimble Navigation Limited, 485 Potrero Avenue, Sunnyvale, CA 94086. (e-mail: grant_marshall@trimble.com)

(Received August 30, 1995; revised May 9, 1996; accepted May 17, 1996.)